Applied Surface Science 264 (2013) 433–442

Contents lists available at SciVerse ScienceDirect

Applied Surface Science

journal homepage: www.elsevier.com/locate/apsusc

Effect of the surface oxygen groups on methane adsorption on coals

Shixiong Hao[a,b], Jie Wen[a], Xiaopeng Yu[a,b], Wei Chu[a,*]

[a] Department of Chemical Engineering, Sichuan University, Chengdu 610065, China
[b] Department of Chemical Engineering, Sichuan University of Science & Engineering, Zigong 643000, China

ARTICLE INFO

Article history:
Received 6 July 2012
Received in revised form
26 September 2012
Accepted 8 October 2012
Available online 16 October 2012

Keywords:
Coal
Surface oxygen groups
Methane
Adsorption

ABSTRACT

To investigate the influence of surface oxygen groups on methane adsorption on coals, one bituminous coal was modified with H_2O_2, $(NH_4)_2S_2O_8$ and HNO_3 respectively, to prepare coal samples with different surface properties. The oxygen groups on coal surface were characterized by X-ray photoelectron spectroscopy (XPS). The textures of the coal samples were investigated by N_2 adsorption at 77 K. Their surface morphologies were analyzed by scanning electron microscopy (SEM). The methane adsorption behaviors of these coal samples were measured at 303 K in pressure range of 0–5.3 MPa by volumetric method. The adsorption data of methane were fitted to the Langmuir model and Dubinin–Astakhov (D–A) model. The fitting results showed that the D–A model fitted the isotherm data better than the Langmuir model. It was observed that there was, in general, a positive correlation between the methane saturated adsorption capacity and the micropore volume of coals while a negative correlation between methane saturated adsorption capacity and the O_{total}/C_{total}. The methane adsorption capacity was determined by the coal surface chemistry when the microporosity parameters of two samples were similar. Coal with a higher amount of oxygen surface groups, and consequently with a less hydrophobic character, had lower methane adsorption capacity.

1. Introduction

Coal is a source, reservoir and trap for significant quantities of methane and minor amounts of other gases. This gas, referred to as coalbed methane (CBM), generally consists of a mixture of CH_4 (95–98%), CO_2, N_2 and higher hydrocarbons (C_2—C_5) [1]. Worldwide CBM resources are estimated to range between 84.2 and 358.2×10^{12} m^3 [2]. Thus, CBM is potentially an important economic resource. Besides, CBM is an explosive and outburst hazard during underground mining, and its leakage to the atmosphere contributes to the greenhouse effect. The adsorption of methane on coals is an important research area. Adsorption and desorption isotherms can be used to evaluate potential storage of CBM, to enhance gas recovery from coal seams and to assist the understanding of gas-related problems in underground coal mining such as explosive and outburst hazard.

Attempts were made to find a relationship between coal properties and methane adsorption capacity [3–11], but many studies were contradictory and many empirical relationships developed for particular basins could not be readily applied elsewhere [4]. Bustin and Clarkson [4] investigated the influence of coal rank on methane reservoir capacity for a series of Australian, Canadian and American coals and found that there was no or little correlation between coal rank and methane adsorption capacity, although in particular basins there were general trends with coal rank. However, Laxminarayana and Crosdale [9] found that the methane adsorption capacity followed a second-order polynomial trend with rank (0.62% up to 1.46% R_0 max) and coalification as the primary composition of the coal had a significant influence on the pore structure and therefore on the adsorption capacity. Some researches into the effect of petrographic composition on CH_4 adsorption capacity found that bright coals had a higher capacity than dull coals at the same rank [4,8,10]. However, some investigations revealed that there was no correlation between adsorption capacity and maceral composition [9,11].

Therefore, although CH_4 adsorption onto coal has been studied for many years, the factors influencing the methane adsorption still call for further investigation. The adsorption ability of adsorbent is associated with its physical and chemical properties [12,13]. The surface characteristics of carbon materials depend on the content of heteroatoms, such as oxygen or nitrogen which determine the charge, hydrophobicity, and electronic density of the grapheme layers [13]. It is well known that oxygen is the most abundant heteroatom in coals and exists in oxygen functional groups such as the hydroxyl groups (predominantly phenolic), carboxyl groups, methoxyl groups and carbonyl groups [14,15]. The influence of oxygen functional groups on the methane adsorption capacity of activated carbon has been reported [16]. However, to

* Corresponding author. Tel.: +86 28 85403836; fax: +86 28 85461108.
E-mail address: chuwei1965_scu@yahoo.com (W. Chu).

0169-4332/$ – see front matter © 2012 Elsevier B.V. All rights reserved.
http://dx.doi.org/10.1016/j.apsusc.2012.10.040

Table 1
Proximate and ultimate analysis of the starting coal.

Proximate analysis wt.%				Ultimate analysis wt.%				
Ash	VM	FC	Moisture	C	H	O	N	S
15.53	30.29	69.71	0.99	83.77	6.72	8.05	1.46	Not detected

Ash was calculated on a dry basis. Volatile matter (VM) and fixed carbon (FC) were calculated on a dried, ash-free basis.

our knowledge, no study has been reported on investigating the influence of oxygen functional groups of coals on methane adsorption. A proper understanding of the effect of coal surface chemistry on methane adsorption is critical for the CBM reserves estimation and preventing from its explosive during underground mining. For this purpose, it is necessary to develop coals with similar textural properties but different surface chemistry.

In this paper, we modified one bituminous coal with 30 vol.% H_2O_2, saturated $(NH_4)_2S_2O_8$ solution, 2 mol/L and 4 mol/L HNO_3 solution, respectively, to prepare coal samples with similar porous texture but different surface chemistry. The oxygen complexes on coal surface were characterized by X-ray photoelectron spectroscopy (XPS). The coal texture was determined by N_2 adsorption–desorption at 77 K. The data of methane adsorption equilibrium were measured by volumetric method and fitted to the Langmuir model and Dubinin–Astakhov (D–A) model respectively. The relationship between the microporosity, oxygen functional groups and the methane adsorption capacity were studied.

2. Experimental

2.1. Sample preparation

One bituminous coal from Yihai coal field in Qinghai province (China) was used as the starting material for this study. Proximate analysis and ultimate analysis for the starting coal are given in Table 1. The coal was crushed to particles with size of 60–80 mesh. The as-prepared coal particles were demineralized by mixed acid composed of 45 vol.% HCl, 15 vol.% HF and 40 vol.% H_2O at 343 K for 5 h, then filtrated, washed with deionized water to neutral pH, and dried in an oven overnight at 383 K. This sample was labeled as Coal-O.

Three methods were used to modify the sample Coal-O in order to obtain coal samples with different surface chemistries while maintaining the original textural properties: (a) 30 vol.% hydrogen peroxide was added to Coal-O, at the solid-to-liquid ratio of 1 g: 10 mL, at room temperature and kept for 24 h (sample labeled as Coal-HP); (b) ammonium persulfate saturated solution was added to Coal-O, at the solid-to-liquid ratio of 1 g: 20 mL, at room temperature and kept for 24 h (sample labeled as Coal-APS); (c) 2 mol/L and 4 mol/L nitric acid were added to Coal-O, at the solid-to-liquid ratio of 1 g: 10 mL, at room temperature and kept for 24 h respectively (samples labeled as Coal-NA2 and Coal-NA4 respectively). After modification, all the samples were washed with deionized water to neutral pH, dried in the oven overnight at 383 K and then stored in a desiccator.

2.2. Characterization

The textural characterization of the coal samples was based on N_2 adsorption isotherms, determined at 77 K with a NOVA1000e surface area and pore size analyzer (Quantachrome Company). Samples were degassed at 383 K for 24 h prior to the analysis. The specific surface area was calculated by the BET method [17–19]; the micropore volume was determined by the Dubunin–Radushkevich (D–R) equation [18,19]; the total pore volume V_t was evaluated from the nitrogen adsorption at $p/p^0 = 0.98–0.99$ (p and p^0 denote the equilibrium and saturation pressure of nitrogen at 77 K, respectively) [20]; and the pore size distribution was calculated from the D–A method [21–23].

Surface morphology was investigated by scanning electron microscopy (SEM) (JEOL/EO JSM-5900 microscope).

The proximate analysis was investigated by a GF-A6 automatic proximate analyzer (Hebi Celestica Instruments Co., Ltd). The elemental analysis of samples was performed in a Carlo Erba 1106 element analyzer. The oxygen content was determined by difference [24].

X-ray photoelectron spectra technology was used to study the surface composition of coal samples. The experiments were performed on a XSAM 800 spectrometer with an Al Kα($h\nu$ = 1486.6 eV) X-ray source. Charging effects were corrected by adjusting the binding energy of C1s peak from carbon contamination to 284.6 eV [25].

2.3. Adsorption of methane

The adsorption isotherms were obtained through an equilibrium volumetric method. A schematic arrangement is shown in Fig. 1. The precision of the high-precision pressure transducer is 0.05% of the full scale value (maximum pressure 10 MPa). The lines exposed to air were wrapped with heating tape controlled by a PID controller. A brief description is given below.

2.3.1. Helium calibration of free space of adsorption cell

The free space in the adsorption cell was corrected by the helium expansion. Before the helium was entered into theadsorption apparatus, the sample (about 5 g) was evacuated in the adsorptioncell for 24 h at 353 K. After that, the adsorption system was cooled to 303 K (±0.1 K). When the reference cell and adsorption cell temperatures were stable at 303 K (±0.1 K), V1, V2, V4, V5, V6, and V7 were closed. Meanwhile, V3 was kept opened. Then helium gas cylinder regulator and V1 were opened slowly in turn, and pure helium (99.999%) was dosed into the reference cell. After the pressure of the reference cell reached a deserved value, helium gas cylinder regulator, V1 and V3 were closed. When the pressure of the reference cell held steady and was recorded, $p_{ini,1}$, V4 was opened and the gas was transferred into the adsorption cell from the reference cell. When the data from the pressure transducer remained the same for more than 30 min, the system was identified as reaching adsorption equilibrium and the pressure of the reference or adsorption cell was recorded, $p_{equ,1}$. The amount of the gas that transferred from reference cell to the adsorption cell could be calculated from the mass balance between the initial and the equilibrium state. To obtain another group of p_{ini} and p_{equ}, the V4 was closed and then helium gas cylinder regulator, the V1 and V3 were opened again. Then pure helium was dosed into the reference cell till a higher deserved pressure. When the deserved pressure of the reference cell reached, helium gas cylinder regulator, V1 and V3 were closed. Similarly, when the pressure held steady, another initial pressure, $p_{ini,2}$, was obtained. Then V5 was opened and the gas was transferred into the adsorption cell from the reference cell again. When the system reached equilibrium, another equilibrium pressure, $p_{equ,2}$, was obtained. The same procedure was repeated to obtain various groups of $p_{ini,i}$ and $p_{equ,i}$.

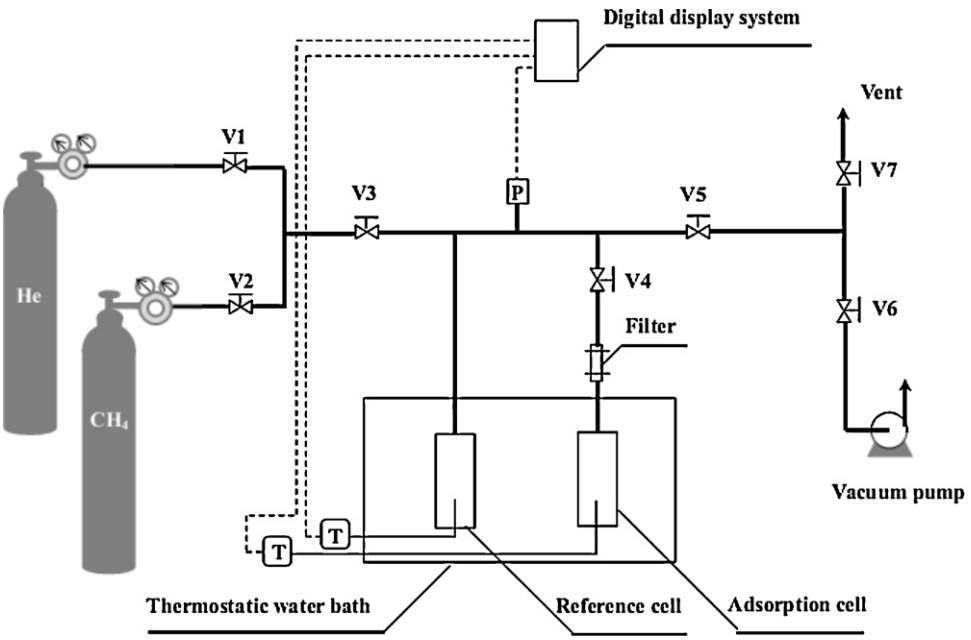

Fig. 1. Schematic arrangement of the experimental set up (V, needle valve; P, pressure transducer; T, thermocouple).

Each of the tests was operated twice to ensure the validity of the experiment.

2.3.2. Methane isotherm

The measurement of methane isotherm was similar to that of the helium calibration in general. The difference is merely that the helium was replaced by methane with a purity of 99.99%.

2.3.3. Data reduction

The helium and methane densities at a given T and p in the gas phase were obtained from the NIST website [26,27].

The free space volume of the adsorption cell is calculated as follows,

$$m^{\mathrm{He}}_{\mathrm{transfered}} = \sum_{i=1}^{N} V_{\mathrm{ref}} \cdot \left[\rho^{\mathrm{He}}(p_{\mathrm{ini},i}, T) - \rho^{\mathrm{He}}(p_{\mathrm{equ,i}}, T)\right] \quad (1)$$

where $m^{\mathrm{He}}_{\mathrm{transfered}}$ is the mass of helium gas that transferred from the reference cell to the adsorption cell during N successive pressure steps (in g); V_{ref} is the volume of the reference cell (in cm^3); $\rho^{\mathrm{He}}(p_{\mathrm{ini},i}, T)$ and $\rho^{\mathrm{He}}(p_{\mathrm{equ},i}, T)$ are the density of helium gas in the reference cell at each initial and adsorption equilibrium state respectively(in $\mathrm{g\,cm}^{-3}$).

Since the helium is not adsorbed in the coal ($p < 10$ MPa) [28], the amount of helium transferred is the same as the amount of helium in the free space of the adsorption cell.

$$m^{\mathrm{He}}_{\mathrm{transfered}} = V_{\mathrm{free}} \cdot \rho^{\mathrm{He}}(p_{\mathrm{equ},N}, T) \quad (2)$$

$$V_{\mathrm{free}} = \frac{m^{\mathrm{He}}_{\mathrm{transfered}}}{\rho^{\mathrm{He}}(p_{\mathrm{equ},N}, T)} \quad (3)$$

where V_{free} is the volume of free space in the adsorption cell after one coal sample dosed (in cm^3); ρ^{He} ($p_{\mathrm{equ},N}$, T) is the density of helium gas in the reference cell at Nth equilibrium state (in $\mathrm{g\,cm}^{-3}$). Repeating the helium dosing and outgassing process for the reference cell, the V_{free} at different equilibrium pressure could be obtained, and their mean value was used to calculate the methane adsorption data.

The amount of methane gas that transferred from reference cell to adsorption cell during N successive pressure steps ($m^{\mathrm{gas}}_{\mathrm{transfered}}$, in g) was calculated by the following equation:

$$m^{\mathrm{gas}}_{\mathrm{transfered}} = \sum_{i=1}^{N} V_{\mathrm{ref}} \cdot \left[\rho^{\mathrm{gas}}(p_{\mathrm{ini},i}, T) - \rho^{\mathrm{gas}}(p_{\mathrm{equ},i}, T)\right] \quad (4)$$

where ρ^{gas} ($p_{\mathrm{ini},i}$, T) and $\rho^{\mathrm{gas}}(p_{\mathrm{equ},i}, T)$ are the density of methane gas in the reference cell at each initial and adsorption equilibrium state respectively (in $\mathrm{g\,cm}^{-3}$).

After N successive pressure steps, the methane transferred from reference cell to the adsorption cell was partly adsorbed in the micro- and mesopores of the adsorbent, and the leftover gas occupied the residual free space [18], namely ($V_{\mathrm{free}} - V_{\mathrm{adsorbed}}$), where V_{adsorbed} is the volume of the adsorbed phase. Thus, the adsorbed mass (m_{adsorbed}), also named as absolute adsorbed mass (m_{absolute}), could be calculated by follow equations.

$$m_{\mathrm{adsorbed}} = m^{\mathrm{gas}}_{\mathrm{transfered}} - \rho^{\mathrm{gas}}(p_{\mathrm{ads\_cell}}, T) \cdot (V_{\mathrm{free}} - V_{\mathrm{adsorbed}}) \quad (5)$$

where ρ^{gas} ($p_{\mathrm{ads\_cell}}$, T) is the density of methane gas in the adsorption cell at the pressure $p_{\mathrm{ads\_cell}}$ (which is system equilibrium pressure at Nth equilibrium state i.e. $p_{\mathrm{equ},N}$) and the temperature T (303 K).

As the V_{adsorbed} cannot be determined directly, the V_{free} is used to substitute for the residual free space ($V_{\mathrm{free}} - V_{\mathrm{adsorbed}}$) in volumetric method experiment. Then so-called excess adsorption mass (m_{excess}) could be approached by following equation,

$$m_{excess} = m^{gas}_{transfered} - \rho^{gas}(p_{ads\_cell}, T) \cdot V_{free} \quad (6)$$

However, all the conventional isotherm equations were originally derived for m_{adsorbed}, therefore it should be m_{adsorbed} rather than m_{excess} to be applied for evaluating the thermodynamic property of adsorbed phase [29].

From the Eqs. (5) and (6), the following equation could be obtained,

$$m_{\mathrm{excess}} = m_{\mathrm{adsorbed}} - \rho^{\mathrm{gas}}(p_{\mathrm{ads\_cell}}, T) \cdot V_{\mathrm{adsorbed}} \quad (7)$$

While

$$m_{\mathrm{adsorbed}} = \rho_{\mathrm{adsorbed}} \cdot V_{\mathrm{adsorbed}} \quad (8)$$

where $\rho_{adsorbed}$ is the density of the adsorbed phase (in g cm^{-3}).

Therefore

$$m_{adsorbed} = \frac{m_{excess}}{1 - (\rho^{gas}(p_{ads\_cell}, T)/\rho_{adsorbed})} \quad (9)$$

The higher equilibrium pressures, the larger value of $(\rho^{gas}(p_{ads\_cell}, T)/\rho_{adsorbed})$, and the difference between m_{excess} and $m_{adsorbed}$ becomes more apparent. A major problem in determining absolute sorption is that $\rho_{adsorbed}$ cannot be determined directly and certain assumptions have to be made. The density of the adsorbed phase ($\rho_{adsorbed}$) is estimated by the following equation [18,30].

$$\rho_{adsorbed} = \rho_b \exp[-\alpha(T - T_b)] \quad (10)$$

where ρ_b is the density of the liquid methane at the normal boiling point (0.42235 g/cm^3); T_b is normal boiling point of methane (111.67 K); and α is the thermal expansion coefficient of the adsorbed phase that can be expressed as follows [18,31,32].

$$\alpha = \frac{1}{v_{adsorbed}} \left(\frac{\partial v_{adsorbed}}{\partial T} \right) \approx \frac{1}{T} \quad (11)$$

where $v_{adsorbed}$ is the adsorbed phase specific volume equal to $1/\rho_{adsorbed}$ (in cm^3 g^{-1}).

The specific adsorbance, n (in mmol g^{-1}), is given by

$$n = \frac{m_{adsorbed} \times 1000}{M_{CH_4} \times m_{sample}} \quad (12)$$

where m_{sample} is the mass of coal sample in the adsorption cell (in g); M_{CH_4} is molecular weight of methane (in g mol^{-1}).

2.3.4. Isotherm correlations

The Langmuir and the D–A models, which have been widely used for IUPAC Type I isotherms [33,34], were used to correlate the experimental equilibrium data. In the CBM industry and related reservoir simulations approaches, the Langmuir model is used as a simple method and provides a reasonable fit to most experimental data [28]. The form of the Langmuir equation used herein is expressed as [35]

$$\frac{n}{n_0} = \frac{bp}{1 + bp} \quad (13)$$

where n_0 is the maximum adsorption capacity (in mmol g^{-1}); p is the equilibrium pressure (absolute pressure in MPa); b is the Langmuir constant (in M Pa^{-1}). n_0, and b are the adsorption parameters that are optimized from the least-squares criteria using the experimental data.

The D–A model for adsorption of gases onto nonhomogeneous carbonaceous solids could account for surface heterogeneity and is expressed as [18,35]

$$\frac{W}{W_0} = \exp\left[-\left(\frac{RT}{E} \ln\left(\frac{p_s}{p} \right) \right)^t \right] \quad (14)$$

where W is the volume of methane adsorbed at equilibrium (in cm^3 g^{-1}); W_0 is the maximum volume that the methane can occupy in the adsorbent (in cm^3 g^{-1}); E is the characteristic energy of the adsorption system (in J mol^{-1}); R is the gas constant; and t is the structural heterogeneity parameter.

Eq. (14) when written in terms of amount adsorbed (mmol g^{-1}) is [18,32,35]:

$$\frac{n}{n_0} = \exp\left[-\left(\frac{RT}{E} \ln\left(\frac{p_s}{p} \right) \right)^t \right] \quad (15)$$

Since the measurements are above the critical point of methane, the following equation suggested by Dubinin [31,36] is applied for calculating the quasi-saturated vapor pressure (p_s) which was proved to be more accurate [37].

$$p_s = p_c \left(\frac{T}{T_c} \right)^2 \quad (16)$$

where the subscript c refers to the critical point (for methane, p_c is 4.5992 MPa, and T_c is 190.56 K). In this case n_0, E, and t are the adsorption parameters which are optimized from the least-squares criteria.

The prediction uncertainty is determined by the mean relative deviation δ:

$$\delta = \sqrt{\frac{1}{N} \sum_{i=1}^{N} \left(\frac{n_i - n_{cal,i}}{n_i} \right)^2} \quad (17)$$

where N is the number of data points.

3. Results and discussion

3.1. Textural characterization

Table 2 summarizes the textural parameters calculated from the nitrogen isotherms such as specific surface area, total pore volume and micropore volume for the samples. The pore size distributions are presented in Fig. 2. As shown in Table 2, the oxidation with H_2O_2 or $(NH_4)_2S_2O_8$ or 2 mol/L HNO_3 did not change the coal texture to large extent, although the surface area, total pore volume and micropore volume slightly decreased as a result of oxidation. From Fig. 2, it can be observed that the Coal-O, Coal-HP, Coal-APS and Coal-NA2 have similar pore size distribution. However, the pore size distribution of the Coal-NA4 is significantly different from the others.

As expected, nitric acid is a strong oxidizing agent and the higher its concentration is, the stronger its oxidation is. After oxidative modification with 4 mol/L HNO_3, the S_{BET}, V_t and V_{mic} decreased by 72.3%, 69.8% and 67.1% respectively. By contrast, the S_{BET}, V_t and V_{mic} of Coal-HP dropped by 11.2%, 12.7% and 11.3% respectively

Table 2
Textural characteristics of the coal samples.

Sample	S_{BET} (m^2/g)	V_t (mm^3/g)	V_{mic} (mm^3/g)
Coal-O	3.722	3.904	0.5628
Coal-HP	3.304	3.409	0.4992
Coal-APS	3.117	3.331	0.4794
Coal-NA2	2.698	3.210	0.4228
Coal-NA4	1.029	1.179	0.1850

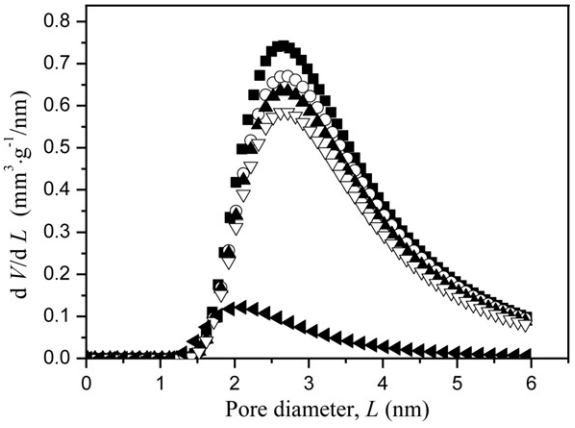

Fig. 2. Pore size distributions obtained by applying the D–A equation to the N_2 adsorption data. ■, Coal-O; ○, Coal-HP; ▲, Coal-APS; ▽, Coal-NA2; and ◄, Coal-NA4.

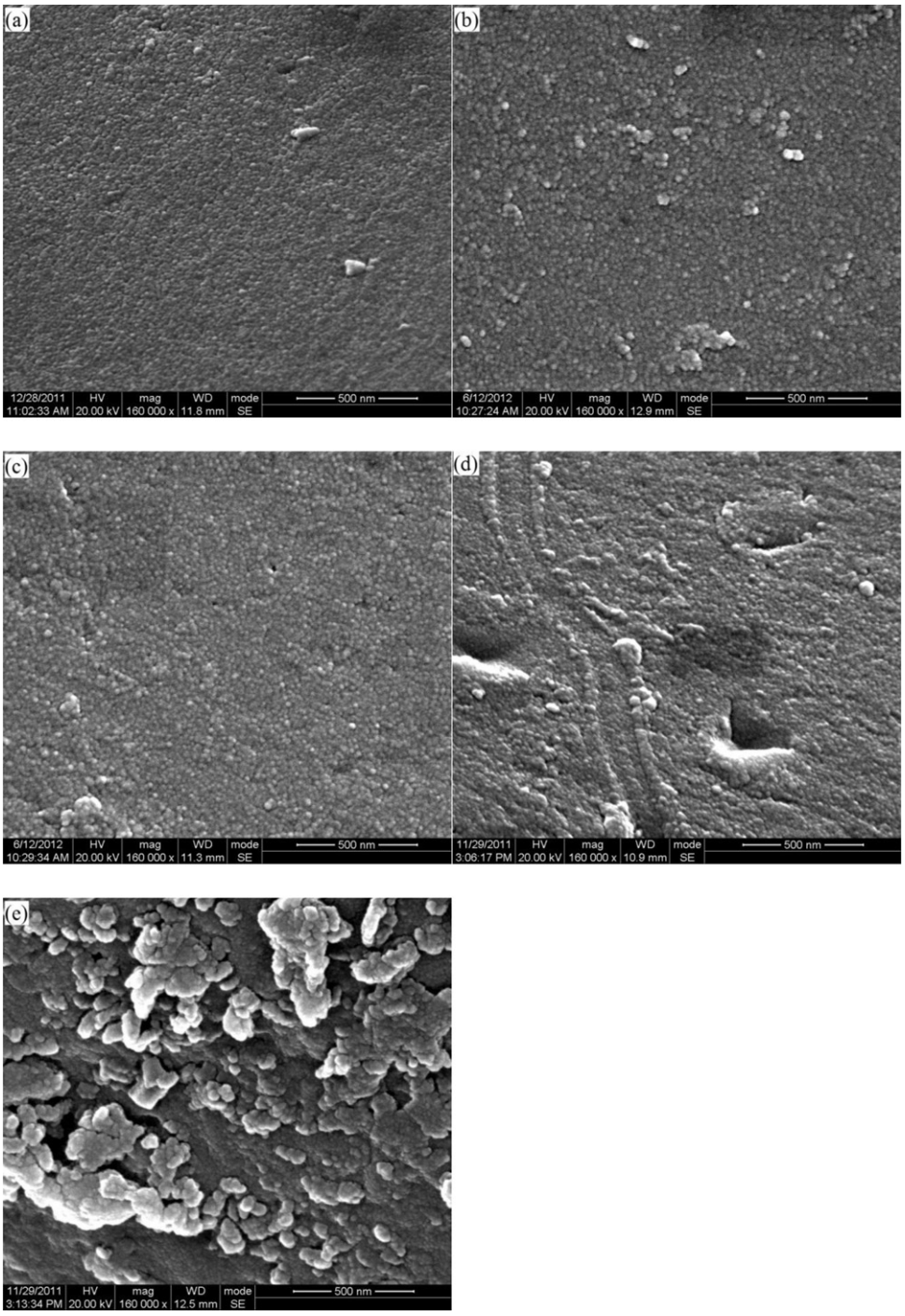

Fig. 3. SEM images of (a) Coal-O, (b) Coal-HP, (c) Coal-APS, (d) Coal-NA2 and (e) Coal-NA4.

when compared with Coal-O. This is because the oxidation of the coal with 4 mol/L HNO_3 introduced more oxygen groups blocking pore entrances and destroyed the pore walls more seriously by removal of carbon atoms from the matrix [38].

Fig. 3 shows the SEM images of these samples. It was observed that the surface morphology of Coal-O, Coal-HP, Coal-APS and Coal-NA2 was similar, while the surface morphology of Coal-NA4 was seriously destroyed after oxidation. The change in the surface morphology is in agreement with the S_{BET} and V_{mic} results of coal samples. The more seriously coal surface is destroyed, the lower S_{BET} or V_{mic} is.

3.2. Proximate and ultimate analysis

The proximate and ultimate analysis of the coal samples are shown in Table 3. The proximate analysis results showed that there was little difference between the Coal-O, Coal-APS, Coal-HP, Coal-NA2 and Coal-NA4. This means that the oxidation treatments used in this paper did not modify the organic composition of coal significantly. The ultimate analysis results showed that oxidative treatments led to the increase in oxygen content. The ascending order of oxygen content in coal samples is Coal-O < Coal-APS < Coal-HP < Coal-NA2 < Coal-NA4.

Table 3
Proximate and ultimate analysis of the coal samples.

Sample	Proximate analysis wt.%				Ultimate analysis wt.%			
	Ash	VM	FC	Moisture	C	H	N	O
Coal-O	2.55	26.49	73.51	1.02	84.66	6.31	1.49	7.54
Coal-HP	2.48	26.36	73.64	1.21	83.65	6.42	1.51	8.42
Coal-APS	2.35	26.23	73.77	0.94	84.19	6.36	1.61	7.84
Coal-NA2	2.21	26.63	73.37	0.28	83.54	6.45	1.53	8.48
Coal-NA4	1.87	28.15	71.85	0.37	79.89	6.51	1.56	12.04

Ash was calculated on a dry basis. Volatile matter (VM) and fixed carbon (FC) were calculated on a dried, ash-free basis.

3.3. Characterization of surface chemistry

Table 4 and Fig. 4 show the XPS results. The content of C, O was calculated from the corresponding peak areas. The ratio of total oxygen to total carbon, O_{total}/C_{total}, which indicates the degree of surface oxidation, was also calculated. For a better understanding of the change in surface chemistry during the modification, the peaks were deconvoluted by XPS Peak 4.1 software, using Shirley's

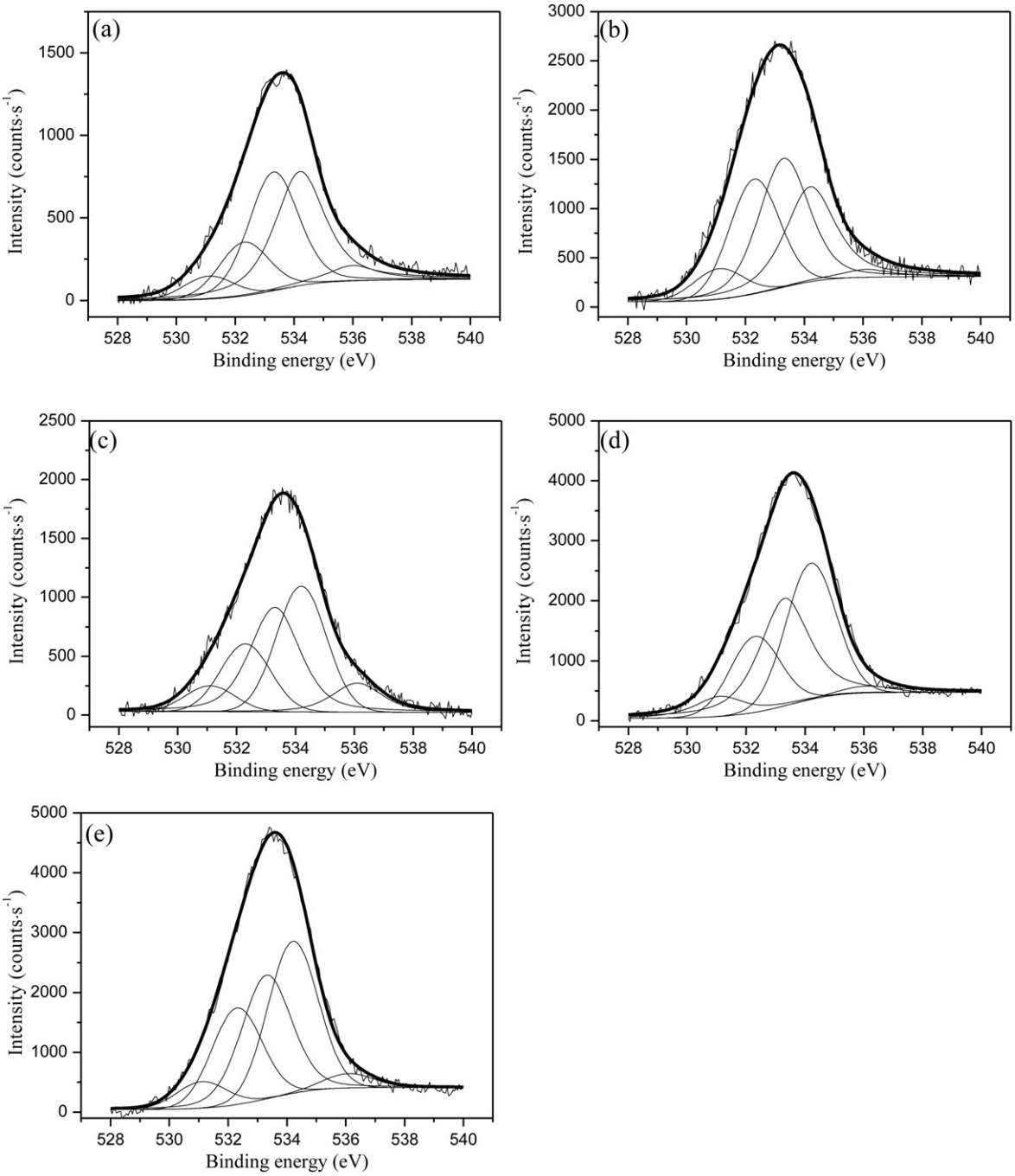

Fig. 4. High resolution XPS spectra for O1s peak and fitting curves of (a) Coal-O, (b) Coal-HP, (c) Coal-APS, (d) Coal-NA2 and (e) Coal-NA4.

Table 4
XPS results for the O1s region, values given in at.% of the total amount.

Sample	Binding energy (eV)					O_{total}/C_{total}
	531.1	532.3	533.3	534.2	536.1	
Coal-O	0.50	1.21	2.83	3.21	0.49	0.0896
Coal-HP	0.76	2.79	3.75	3.07	0.29	0.1203
Coal-APS	0.71	1.92	3.80	3.56	0.38	0.1158
Coal-NA2	0.75	2.16	3.96	3.87	0.19	0.1228
Coal-NA4	0.74	2.69	3.79	4.23	0.40	0.1343

method to correct baseline and fixing the width at half-height equal to 2.0 eV [39,40]. The deconvolution of the O1s spectra yielded the following five peaks [39,40]: peak 1 (531.0–531.9 eV), carbonyl oxygen of quinones; peak 2 (532.3–532.8 eV), carbonyl oxygen atoms in esters, anhydrides and oxygen atoms in hydroxyl groups; peak 3 (533.1–533.8 eV), non-carbonyl (ether- type) oxygen atoms in esters and anhydrides; peak 4 (534.3–535.4 eV), oxygen atoms in carboxyl groups; and peak 5 (536.0–536.5 eV), adsorbed water and/or oxygen.

From Table 4, it was observed that the O_{total}/C_{total} of the samples increased after the oxidative modification which indicated that the oxygen functional groups were introduced onto the coal surface. The O_{total}/C_{total} increased by 34.26%, 29.24%, 37.05% and 49.88% when the Coal-O was modified with H_2O_2, $(NH_4)_2S_2O_8$, 2 mol/L HNO_3 and 4 mol/L HNO_3 respectively. The ascending order of O_{total}/C_{total} of coal samples is Coal-O < Coal-APS < Coal-HP < Coal-NA2 < Coal-NA4, which is consistent with ultimate analysis results. However, the XPS results are not directly comparable with the ultimate analysis techniques, since only the uppermost layer (10–15 nm) are analyzed [39].

The oxidation treatments caused the sample surface becoming more acidic with an increase mainly in peak 2, 3 and 4 which were assigned to esters, anhydrides, hydroxyl and carboxylic acid respectively.

3.4. Adsorption isotherms

Experimentally measured uptake data at 303 K and pressures up to 5.3 MPa for the adsorption of methane on the five samples are shown in Fig. 5. The adsorption isotherms of methane on the samples are of Type I of the IUPAC classification. The isotherm data were regressed using the Langmuir model and D–A model respectively. The solid lines in Fig. 5 represent the isotherms calculated from the Langmuir model using the regressed adsorption parameters (n_0 and b) that are listed in Table 5.

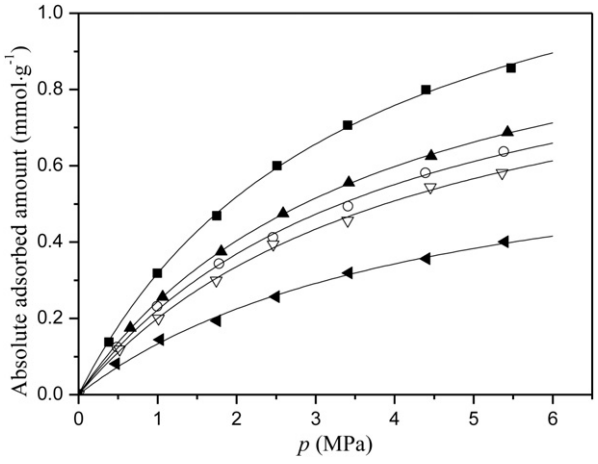

Fig. 5. Adsorption isotherms of methane on: ■, Coal-O; ○, Coal-HP; ▲, Coal-APS; ▽, Coal-NA2; and ◄, Coal-NA4 at 303 K. Solid lines are from the Langmuir model.

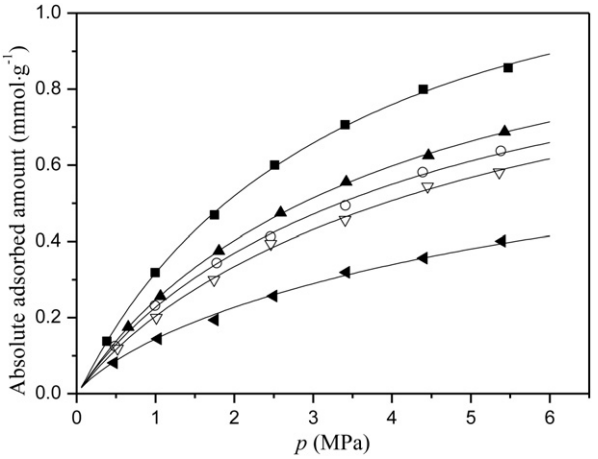

Fig. 6. Adsorption isotherms of methane on: ■, Coal-O; ○, Coal-HP; ▲, Coal-APS; ▽, Coal-NA2; and ◄, Coal-NA4 at 303 K. Solid lines are from the D–A model.

The parameter b is a measure of how strong an adsorbate molecule is attracted onto a surface [35]. When the constant b is larger, the surface is covered more with adsorbate molecules as a result of the stronger affinity of adsorbate molecule toward the surface [35]. Table 5 shows the b and n_0 decrease along with the increase of the O_{total}/C_{total}. The n-alkanes adsorption takes place by only dispersive forces which depend on the polarizability of the molecules [41]. If the value of O_{total}/C_{total} increases, the polarizability of the molecules increases which is unfavorable for adsorption of nonpolar molecule such as methane [16].

Because of its simplicity and providing a reasonable fit to most experimental data, Langmuir model is widely used in the CBM industry and related reservoir simulations approaches [28]. However, the assumption of an energetically homogeneous surface as proposed by Langmuir theory is not true for coal [42]. Fitzgerald et al. [43] proposed simplified local density model (SLD), but this model was not convenient to use. Sakurovs et al. [44] and Kim et al. [26] applied modified D–R equation to model gases adsorption on coals. However, the modified D–R equation is not intuitive for using gas density instead of gas pressure (and adsorbed phase density rather than saturation pressure) to describe gases sorption on coals. Clarkson et al. [42] applied potential theory to the methane-coal system, obtained temperature-invariant methane characteristic curves and found that D–A equation provided a better fit to coal gas isotherm than the Langmuir equation. Similar observations were made by Harpalani et al. [45,46].

The D–A model was employed to fit the uptake data and the results are shown in Fig. 6. The adsorption parameters (n_0, E, and t) and mean relative deviation are listed in Table 6. The solid lines in Fig. 6 represent the isotherms calculated from the D–A model.

The mean relative deviation δ for D–A model is smaller than that for Langmuir model as shown in Table 6. This indicates that the D–A model fitted the experimental data better than the Langmuir model. This finding is in agreement with studies by Clarkson et al. [42], Harpalani et al. [45] and Yu et al. [46].

The parameter t in D–A model describes the surface heterogeneity [35]. If the parameter t of a given system deviates from 3 (usually smaller than 3) more, the system is said to be more heterogeneous [35]. The value of t decreases along with the increase of the O_{total}/C_{total} (see Table 4) in general. This means that the more serious oxidation is, the more heterogeneous the coal surface is. The parameter E in D–A model is characteristic energy which is a measure of the strength of interaction between adsorbate and adsorbent [35]. Table 6 shows the E and n_0 decrease along with the increase of the O_{total}/C_{total}. The higher O_{total}/C_{total} of a sample

Table 5
Adsorption parameters of the Langmuir model for adsorption isotherms of methane on the coals at 303 K.

Langmuir model	Coal-O	Coal-HP	Coal-APS	Coal-NA2	Coal-NA4
n_o (mmol g^{-1})	1.4080	1.0876	1.1554	1.0443	0.7226
b (MPa^{-1})	0.2916	0.2567	0.2688	0.2369	0.2264
Mean relative deviation δ (%)	1.71	2.53	0.65	2.06	6.07

Table 6
Adsorption parameters of the D–A model for adsorption isotherms of methane on the coals at 303 K.

D–A model	Coal-O	Coal-HP	Coal-APS	Coal-NA2	Coal-NA4
n_o (mmol g^{-1})	1.0224	0.7847	0.8398	0.7529	0.520
E (J mol^{-1})	5622.48	5355.35	5412.51	5128.37	5014.20
t	1.6458	1.5004	1.5456	1.4366	1.3253
Mean relative deviation δ (%)	0.89	1.65	0.55	1.87	2.73

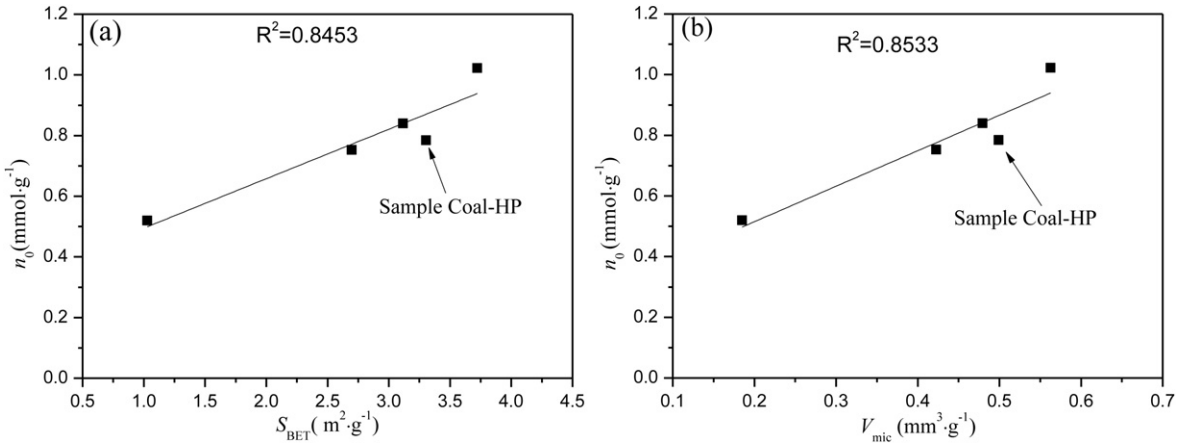

Fig. 7. Saturation adsorption capacity, n_0 (from D–A model) related to the (a) S_{BET} and (b) V_{mic}.

is, the more oxygen groups it has. The oxygen groups may block pore entrances and reduce dispersive interactions of methane with small pore walls [47].

The relationship between n_0 (from D–A model) and S_{BET} is presented in Fig. 7(a). As a general trend, Fig. 7(a) shows that the n_0 is roughly proportional to the S_{BET} of the samples and the correlation coefficient R^2 is 0.8453. The relationship between n_0 and V_{mic} is presented in Fig. 7(b) and the correlation coefficient R^2 is 0.8533. The correlation coefficient between V_{mic} and n_0 is higher than that for S_{BET}. This is because the micropore volume not surface area is a controlling factor on gas sorption on coal [8,23].

However, it should be noted that the sample Coal-HP has a higher V_{mic} but a lower n_0 than the Coal-APS. Bustin and Clarkson [4] found, for a suite of Canadian and Australian coals of similar rank and maceral composition, that those coals with a higher micropore volume (performed on dry coals) have a lower methane adsorption capacity (determined on moisture-equilibrated coals). These indicate that the difference in porosity alone cannot explain the methane adsorption behavior on coals. The samples Coal-HP and Coal-APS have similar texture properties, but different oxygen content. The O_{total}/C_{total} of the sample Coal-HP is higher than that of the Coal-APS. The n-alkanes adsorption takes place by only dispersive forces which depend on the polarizability of the molecules [41]. With similar textural properties, the samples with higher percentages of O_{total}/C_{total} should exhibit a lower adsorption capacity for a nonpolar molecule such as methane [16].

Fig. 8 shows the relationship between n_0 (from D–A model) and O_{total}/C_{total}. It was observed that the n_0 was roughly inverse proportional to the O_{total}/C_{total} of the samples as a general trend. However, there is a little deviation from the tendency line identified in Fig. 8 for the sample Coal-NA4. This may be attributed to there being a big difference in S_{BET} or V_{mic} between the sample Coal-NA4 and the other samples. The S_{BET} and V_{mic} of sample Coal-NA4 are only 38.14%, 43.76% of the sample Coal-NA2 respectively (see Table 2).

Coal is porous material. Gas may be retained in the coalbed reservoir in several forms [23]: (1) free (gas in excess of that which can be adsorbed, in the cleats, fractures and porosity of the coal); (2) as a solute in groundwater occupying the coal reservoir; and (3) adsorbed on the internal surfaces (e.g. in micropores). The third type, adsorbed gas, is the primary source of methane gas retention in coal [23]. Therefore, the study of coal pore characteristics

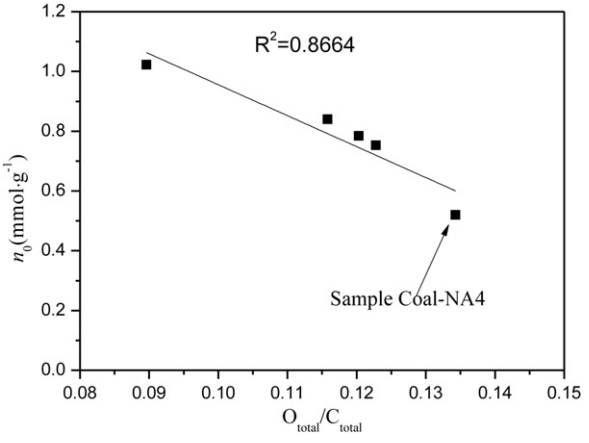

Fig. 8. Saturation adsorption capacity, n_0 (from D–A model) related to O_{total}/C_{total}.

has been important basic research. However, Bustin and Clarkson's [4] and our findings indicated that the difference in porosity alone cannot explain the methane adsorption behavior on coals. Consequently, not only pore structure of coal should be considered but also its surface characteristics when evaluating coalbed methane reserves. In addition, our results showed that the S_{BET} or V_{mic} of coal would decrease, and O_{total}/C_{total} would increase after oxidation. The decrease of V_{mic} and increase of O_{total}/C_{total} would decrease the saturated adsorption capacity of coal, and then promote the desorption of methane. So, it may be considered to inject H_2O_2 into coal seam to improve coalbed methane recovery rate.

4. Conclusion

In this work, one bituminous coal has been modified using four oxidation agents. The N_2 adsorption isotherms indicated that they possessed similar porous texture except for sample Coal-NA4. X-ray photoelectron spectra data showed that the oxygen functional groups were introduced on the coal surfaces and their contents in the coals are in the order of Coal-NA4 > Coal-NA2 > Coal-HP > Coal-APS > Coal-O.

The methane adsorption capacities of the coals were tested by volumetric method and fitted by the Langmuir model and the D–A model. The fitting results showed that (i) the D–A model fitted the isotherm data better than the Langmuir model; (ii) there was, in general, a positive correlation between methane adsorption capacity and the micropore volume; (iii) the adsorption capacity of methane depended on the surface chemistry of the samples when the microporosity parameters of two samples were similar. Coals with a higher amount of oxygen surface groups, and therefore, with a lower hydrophobic property, have lower methane adsorption capacity.

Acknowledgments

This work was supported by the National Basic Research Program of China (973 Program, No. 2011CB201202) and the National Natural Science Foundation of China (20776089).

The authors also thank Jingjie Luo, Wenjing Sun, Ning Wang and Lihong Huang for their helpful discussions.

References

[1] H. Yu, L. Zhou, W. Guo, J. Cheng, Q. Hu, Predictions of the adsorption equilibrium of methane/carbon dioxide binary gas on coals using Langmuir and ideal adsorbed solution theory under feed gas conditions, International Journal of Coal Geology 73 (2008) 115–129.
[2] P. Weniger, W. Kalkreuth, A. Busch, B.M. Krooss, High-pressure methane and carbon dioxide sorption on coal and shale samples from the Parana Basin, Brazil, International Journal of Coal Geology 84 (2010) 190–205.
[3] J.H. Levy, S.J. Day, J.S. Killingley, Methane capacities of Bowen basin coals related to coal properties, Fuel 76 (1997) 813–819.
[4] R. Bustin, C. Clarkson, Geological controls on coalbed methane reservoir capacity and gas content, International Journal of Coal Geology 38 (1998) 3–26.
[5] P.J. Crosdale, B.B. Beamish, M. Valix, Coalbed methane sorption related to coal composition, International Journal of Coal Geology 35 (1998) 147–158.
[6] C. Laxminarayana, P.J. Crosdale, Role of coal type and rank on methane sorption characteristics of Bowen Basin, Australia coals, International Journal of Coal Geology 40 (1999) 309–325.
[7] A. Busch, Y. Gensterblum, B.M. Krooss, Methane and CO_2 sorption and desorption measurements on dry Argonne premium coals: pure components and mixtures, International Journal of Coal Geology 55 (2003) 205–224.
[8] M. Mastalerz, H. Gluskoter, J. Rupp, Carbon dioxide and methane sorption in high volatile bituminous coals from Indiana, USA, International Journal of Coal Geology 60 (2004) 43–55.
[9] C. Laxminarayana, P.J. Crosdale, Controls on methane sorption capacity of Indian coals, AAPG Bulletin 86 (2002) 201–212.
[10] A. Hildenbrand, B.M. Krooss, A. Busch, R. Gaschnitz, Evolution of methane sorption capacity of coal seams as a function of burial history – a case study from the Campine Basin, NE Belgium, International Journal of Coal Geology 66 (2006) 179–203.
[11] M. Faiz, A. Saghafi, N. Sherwood, I. Wang, The influence of petrological properties and burial history on coal seam methane reservoir characterisation, Sydney Basin, Australia, International Journal of Coal Geology 70 (2007) 193–208.
[12] X. Lu, J. Jiang, K. Sun, X. Xie, Y. Hu, Surface modification, characterization and adsorptive properties of a coconut activated carbon, Applied Surface Science 258 (2012) 8247–8252.
[13] A. Derylo-Marczewska, B. Buczek, A. Swiatkowski, Effect of oxygen surface groups on adsorption of benzene derivatives from aqueous solutions onto active carbon samples, Applied Surface Science 257 (2011) 9466–9472.
[14] L. Giroux, J.P. Charland, J.A. MacPhee, Application of thermogravimetric Fourier transform infrared spectroscopy (TG-FTIR) to the analysis of oxygen functional groups in coal, Energy Fuels 20 (2006) 1988–1996.
[15] S.R. Kelemen, P.J. Kwiatek, Quantification of organic oxygen species on the surface of fresh and reacted Argonne Premium coal, Energy Fuels 9 (1995) 841–848.
[16] M. Bastos-Neto, D.V. Canabrava, A.E.B. Torres, E. Rodriguez-Castellon, A. Jimenez-Lopez, D.C.S. Azevedo, C.L. Cavalcante, Effects of textural and surface characteristics of microporous activated carbons on the methane adsorption capacity at high pressures, Applied Surface Science 253 (2007) 5721–5725.
[17] J. Xu, W. Chu, S. Luo, Synthesis and characterization of mesoporous V-MCM-41 molecular sieves with good hydrothermal and thermal stability, Journal of Molecular Catalysis A: Chemical 256 (2006) 48–56.
[18] K.A. Rahman, W.S. Loh, H. Yanagi, A. Chakraborty, B.B. Saha, W.G. Chun, K.C. Ng, Experimental adsorption isotherm of methane onto activated Carbon at sub- and supercritical temperatures, Journal of Chemical & Engineering Data 55 (2010) 4961–4967.
[19] T. Garcia, R. Murillo, D. Cazorla-Amoros, A.M. Mastral, A. Linares-Solano, Role of the activated carbon surface chemistry in the adsorption of phenanthrene, Carbon 42 (2004) 1683–1689.
[20] V.M. Gun'ko, Y.V. Zaulychnyy, B.I. Ilkiv, V.I. Zarko, Y.M. Nychiporuk, E.M. Pakhlov, Y.G. Ptushinskii, R. Leboda, J. Skubiszewska-Zieba, Textural and electronic characteristics of mechanochemically activated composites with nanosilica and activated carbon, Applied Surface Science 258 (2011) 1115–1125.
[21] A. Gil, S.A. Korili, G.Y. Cherkashinin, Extension of the Dubinin–Astakhov equation for evaluating the micropore size distribution of a modified carbon molecular sieve, Journal of Colloid and Interface Science 262 (2003) 603–607.
[22] J. Luo, Y. Liu, C. Jiang, W. Chu, J. Wen, H. Xie, Experimental and modeling study of methane adsorption on activated carbon derived from anthracite, Journal of Chemical & Engineering Data 56 (2011) 4919–4926.
[23] C.R. Clarkson, R.M. Bustin, Variation in micropore capacity and size distribution with composition in bituminous coal of the Western Canadian Sedimentary Basin – implications for coalbed methane potential, Fuel 75 (1996) 1483–1498.
[24] M.G. Plaza, F. Rubiera, J.J. Pis, C. Pevida, Ammoxidation of carbon materials for CO_2 capture, Applied Surface Science 256 (2010) 6843–6849.
[25] N. Wang, W. Chu, T. Zhang, X.-S. Zhao, Manganese promoting effects on the Co-Ce-Zr-Ox nano catalysts for methane dry reforming with carbon dioxide to hydrogen and carbon monoxide, Chemical Engineering Journal 170 (2011) 457–463.
[26] H.J. Kim, Y. Shi, J. He, H.-H. Lee, C.-H. Lee, Adsorption characteristics of CO_2 and CH_4 on dry and wet coal from subcritical to supercritical conditions, Chemical Engineering Journal 171 (2011) 45–53.
[27] NIST, Thermophysical properties of fluid systems, http://webbook.nist.gov/chemistry/fluid/
[28] A. Busch, Y. Gensterblum, CBM and CO2-ECBM related sorption processes in coal: a review, International Journal of Coal Geology 87 (2011) 49–71.
[29] L. Zhou, Y.P. Zhou, M. Li, P. Chen, Y. Wang, Experimental and modeling study of the adsorption of supercritical methane on a high surface activated carbon, Langmuir 16 (2000) 5955–5959.
[30] S. Ozawa, S. Kusumi, Y. Ogino, Physical adsorption of gases at high pressure. IV. An improvement of the Dubinin–Astakhov adsorption equation, Journal of Colloid and Interface Science 56 (1976) 83–91.
[31] B.B. Saha, S. Koyama, I.I. El-Sharkawy, K. Habib, K. Srinivasan, P. Dutta, Evaluation of adsorption parameters and heats of adsorption through desorption measurements, Journal of Chemical & Engineering Data 52 (2007) 2419–2424.
[32] X.L. Wang, J. French, S. Kandadai, H.T. Chua, Adsorption measurements of methane on activated carbon in the temperature range (281 to 343) K and pressures to 1.2 MPa, Journal of Chemical & Engineering Data 55 (2010) 2700–2706.
[33] J. Wen, X. Han, H. Lin, Y. Zheng, W. Chu, A critical study on the adsorption of heterocyclic sulfur and nitrogen compounds by activated carbon: equilibrium, kinetics and thermodynamics, Chemical Engineering Journal 164 (2010) 29–36.
[34] S. Himeno, T. Komatsu, S. Fujita, High-pressure adsorption equilibria of methane and carbon dioxide on several activated carbons, Journal of Chemical & Engineering Data 50 (2005) 369–376.
[35] D.D. Do, Adsorption Analysis: Equilibria and Kinetics, Imperial College Press London, London, 1998.
[36] M. Dubinin, The potential theory of adsorption of gases and vapors for adsorbents with energetically nonuniform surfaces, Chemical Reviews 60 (1960) 235–241.
[37] R.K. Agarwal, J.A. Schwarz, Analysis of high pressure adsorption of gases on activated carbon by potential theory, Carbon 26 (1988) 873–887.
[38] Y. El-Sayed, T.J. Bandosz, Role of surface oxygen groups in incorporation of nitrogen to activated carbons via ethylmethylamine adsorption, Langmuir 21 (2005) 1282–1289.

[39] J.L. Figueiredo, M.F.R. Pereira, M.M.A. Freitas, J.J.M. Orfao, Modification of the surface chemistry of activated carbons, Carbon 37 (1999) 1379–1389.
[40] J.H. Zhou, Z.J. Sui, J. Zhu, P. Li, D. Chen, Y.C. Dai, W.K. Yuan, Characterization of surface oxygen complexes on carbon nanofibers by TPD, XPS and FT-IR, Carbon 45 (2007) 785–796.
[41] M.C. Almazan-Almazan, M. Perez-Mendoza, M. Domingo-Garcia, I. Fernandez-Morales, F. del Rey-Bueno, A. Garcia-Rodriguez, F.J. Lopez-Garzon, The role of the porosity and oxygen groups on the adsorption of n-alkanes, benzene, trichloroethylene and 1,2-dichloro ethane on active carbons at zero surface coverage, Carbon 45 (2007) 1777–1785.
[42] C.R. Clarkson, R.M. Bustin, J.H. Levy, Application of the mono/multilayer and adsorption potential theories to coal methane adsorption isotherms at elevated temperature and pressure, Carbon 35 (1997) 1689–1705.
[43] J.E. Fitzgerald, R.L. Robinson, K.A.M. Gasem, Modeling high-pressure adsorption of gas mixtures on activated carbon and coal using a simplified local-density model, Langmuir 22 (2006) 9610–9618.
[44] R. Sakurovs, S. Day, S. Weir, G. Duffy, Application of a modified Dubinin–Radushkevich equation to adsorption of gases by coals under supercritical conditions, Energy Fuels 21 (2007) 992–997.
[45] S. Harpalani, B.K. Prusty, P. Dutta, Methane/CO_2 sorption modeling for coalbed methane production and CO_2 sequestration, Energy Fuels 20 (2006) 1591–1599.
[46] H. Yu, W. Fan, M. Sun, J. Ye, Study on fitting models for methane isotherms adsorption of coals, Journal of China Coal Society 29 (2004) 463–467.
[47] M.R. Cuervo, E. Asedegbega-Nieto, E. Diaz, S. Ordonez, A. Vega, A.B. Dongil, I. Rodriguez-Ramos, Modification of the adsorption properties of high surface area graphites by oxygen functional groups, Carbon 46 (2008) 2096–2106.